Influence of Ru³⁺ ions at Al/GaAs interface on Schottky diodes

H. Mazari[1,*], Z. Benamara[1,4], K. Ameur[1], N. Benseddik[1], O. Bonnaud[2], R. Olier[3], B. Gruzza[4]

[1]*Laboratoire de Microélectronique Appliquée, Département d'électronique, Université Djillali Liabès de Sidi Bel-Abbes, 22000 Sidi Bel-Abbes, Algérie.*
[2]*Groupe de Microélectronique et de Visualisation, Campus de Beaulieu, 35042, Rennes Cedex, France.*
[3]*UMR CNRS-UBO 652 chimie, électrochimie moléculaire et chimie analytique, Faculté des Sciences et Technique, 6 avenue Victor Le Gorgeu, 29285 Brest, France.*
[4]*Laboratoire des Sciences des Matériaux pour l'Electronique et d'Automatique, Université Blaise Pascal, Les Cézeaux, Clermont II, Aubière Cedex, France.*

Abstract

The current-voltage (I-V) and capacitance voltage (C-V) characteristics of Al/n-GaAs and Al/p-GaAs diodes on GaAs substrate treated by Ru³⁺ ions are investigated and compared with characteristics of GaAs diodes on GaAs untreated substrates. The diodes does not have to show an ideal behaviour of I-V characteristic with an ideality factor of 1.13 and barrier height of 0.85 eV and 0.6 eV for Al/n-GaAs and Al/p-GaAs diodes respectively. The forward bias saturation current found with a big value (10^{-10}A, 10^{-12} A) in the Al/n-GaAs (untreated) Schottky diodes compared with Al/n-GaAs (treated) diodes. Contrary the forward bias saturation current found with a small value (10^{-7} A, 10^{-6} A) in the Al/p-GaAs (untreated) Schottky diodes compared with Al/p-GaAs (treated) diodes. The energy distribution of interface states was determined from the forward bias I(V) characteristics. The interface states density found large in the Al/GaAs (treated by Ru³⁺ ions) structure comparing with the Al/GaAs (untreated) structure.

1. Introduction

The electrical transport across Schottky diodes on epi-GaAs surface it took a considerable importance these last years for the widespread applications in electronics devices (MIS, MESFET, etc.). In general, the performance and reliability of a Schottky diode is drastically influenced by the interface quality between the deposited metal and the semiconductor surface. The performance and reliability of Schottky microwave devices (MESFETs, detectors, mixers, and varactor diodes) depends on the density of interface states, like it depend also of the distribution of each states.

Fermi level pinning in metal/GaAs contacts is a well – established phenomenon. It remains until a present a point of discussion and lot of interpretations were proposed.

On all cases, theories have to explain this following experimental fact: the GaAs/metal Fermi level is pinned. In particular, published results on n-GaAs/Al indicate a

---

*) For Correspondence, Email: h_mazari2005@yahoo.fr

pinning level located at 0.8 eV under the conduction band edge and 0.5 eV above the valence band for p-GaAs/Al [1]. On the other hand, to improve the efficiency of liquid junction solar cells (GaAs-electrolyte) Parkinson and al.[16] suggested a chemical treatment combining the effects of $(KOH+Se^{2-}/Se_2^{2-})$ and $(HCl+Ru^{3+})$ aqueous solutions. The observed improvement of the fill factor of each cells has been interpreted by this author as being due to a decrease of the surface states density and/or to a decrease of the surface recombination velocity. At this stage, it is interesting to evaluate the effect a chemical treatment of $(KOH+Se^{2-}/Se_2^{2-})$ and $(HCl+Ru^{3+})$ aqueous solutions on Schottky barrier heights; thus, we have investigated the behaviour of GaAs/Al contacts. In this paper, we show that a shift of the interface Fermi level can be obtained by means of the treatment prior to metal deposition and a significant increase of the density of interface states. It has been shown that the treatment of GaAs surface results in a significant increase of the density of interface states in MIS devices [7].

2. Method of analysis:

When a metal-semiconductor (MS) contact with an interfacial layer is considered, it is assumed that the forward bias current in a Schottky barrier is due to thermoionic emission current corrected by tunnelling, which is expressed [2] as:

$$I = S A * T^2 \exp(-\chi^{0.5}\delta)\exp\left(-\frac{q\phi_{bn}}{kT}\right)\exp\left(\frac{qV}{nkT}\right) = I_s \exp\left(\frac{qV}{nkT}\right) \qquad (1)$$

The semi-Ln(I) curves gives by extrapolation part of the curve up to zero voltage the current of saturation I_s.
A^*: Richardson constant;
S: diode area;
T: absolute temperature, equal to 300 K;
δ: interfacial layer thickness
χ: mean barrier height presented by the thin interfacial layer;
k: Boltzman constant;
q: electrical charge;
n: ideality factor calculated from the following formula:

$$n = \frac{q}{kT} \cdot \frac{\partial V}{\partial(LnI)} \qquad (2)$$

$\left(\dfrac{1}{C^2}\right)$ versus V and ϕ_{bn} (ϕ_{bp}) is given by the formulas (3) and (4).

$$\frac{1}{C^2} = \frac{2}{S^2 \cdot N_D \cdot \varepsilon_0 \cdot \varepsilon_{SC}} \cdot \left(\Phi_{BN} - V_n + V - \frac{kT}{q} \right) \tag{3}$$

$$\begin{cases} \Phi_{BN} = V_T + V_n + \dfrac{kT}{q} \\[2mm] \Phi_{BP} = -V_T + V_p + \dfrac{kT}{q} \end{cases} \tag{4}$$

$$V_n = \frac{kT}{q} \cdot Ln \frac{N_C}{N_D} \qquad ; \qquad V_p = \frac{kT}{q} \cdot Ln \frac{N_V}{N_A} \tag{5}$$

The value of VT can be obtained from voltage axis intercept of C^{-2} versus V graph provided it is a good straight line.

For metal–insulator–semiconductor (MIS) diode having interface states in equilibrium with the semiconductor, the ideality factor n becomes greater than unity, as proposed by Card and Rhoderick [2], and is given by:

$$n = \left[qN_{ss} + \frac{\varepsilon_s}{W} \right] \frac{\delta}{\varepsilon_i} + 1 \tag{6}$$

where W is the space charge width, N_{ss} is the density of the interface states and ε_s and ε_i are the permittivities of the semiconductor and the interfacial layer respectively.

The evaluation of the interface state energy distribution and relative interfacial layer thickness can be performed using the formula derived by Card and Rhoderick [2] and Kolnik and Ozvold [3]. In this case all of the interface states are in equilibrium with the semiconductor when the diode is forward biased.

The energy of the interface states (n-type semiconductor) with respect to the bottom of the conduction band at the surface of the semiconductor, E_{SS} is given by [4-5]

$$E_c - E_{SS} = q(\phi_{bn} - V) \tag{7}$$

For p-type (with respect to the maximum of the valence band)

$$E_{ss} - E_V = q(\phi_{bp} - |V|) \tag{8}$$

3. Experimental procedure

Schottky contacts were made on (100) polished surface of non-intentionally doped n and p-type GaAs ($N_D, N_A \cong 2 \cdot 10^{16} \, cm^{-3}$). The ohmicity of back contacts was checked before each experiment.

The samples were chemically treated as follows:

1. Cleaning in trichlorethylene, acetone and methanol followed by etching in $H_2SO_4 - H_2O_2 - H_2O$ (5:1:1) at T = 65°C. After these operations, the samples were introduced in a glove box under nitrogen atmosphere;
2. dipping into 1M (Se^{2-}/Se_2^{2-}) solution at pH=14, under illumination (n- GaAs) and in the dark (p-GaAs) for 15 minutes;
3. Dipping into (1M HCL+10^{-2}M Ru^{3+}) solution for 15 minutes.

After each treatment, the samples were rinsed with freshly deionized water. Finally, they were rinsed with methanol.

In the following, the terms: untreated and fully treated samples refer to the samples subjected to the first treatment only and to all three treatments, respectively.
Aluminium depositions were performed by vacuum thermal evaporation on untreated and fully treated samples.

4. Results and discussion

In parallel with the aluminium deposition, the Ru^{3+} adsorption on treated GaAs surfaces was controlled by photoelectrochemical measurements on aqueous (Se^{2-}/Se_2^{2})/GaAs junction [7].
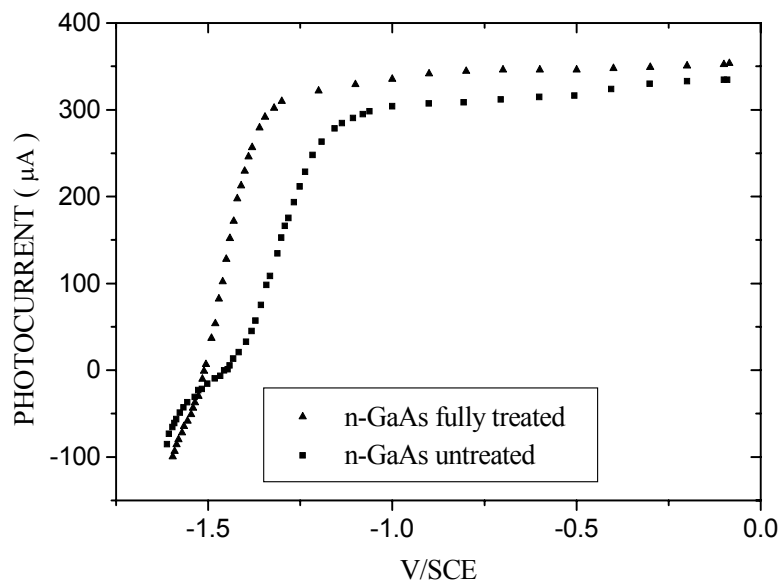

Fig. 1: I-V curves showing the effect of Ru^{3+} treatment on the photoelectrochemical characteristics of n-GaAs in Se^{2-}/Se_2^{2-} -KOH solution. Note the more abrupt rise for the fully treated sample.
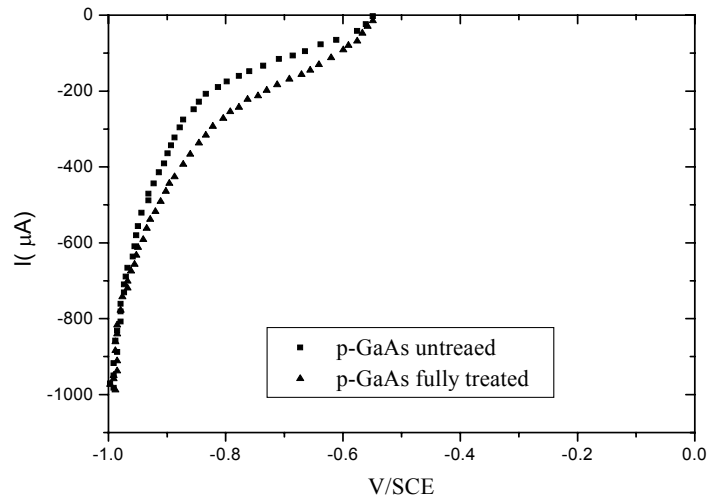
Fig. 2: I-V curves showing the effect of Ru^{3+} treatment on the electrochemical characteristics of p-GaAs in Se^{2-}/Se_2^{2-} -KOH solution.

The effect of a treatment is shown in figure 1 and 2. Figure1 presents the I-V curves showing the effect of Ru^{3+} treatment on the photoelectrochemical characteristics of n-GaAs in Se^{2-}/Se_2^{2-} -KOH solution. We note the more abrupt rise for the fully treated sample. In this figure we may note the more abrupt rise of the photocurrent for the treated sample which is related to the enhancement of the fill factor photoelectrochemical cells [7-11].
Figure2 presents the I-V curves showing the effect of Ru^{3+} treatment on the electrochemical characteristics of p-GaAs in Se^{2-}/Se_2^{2-} -KOH solution. We note an increase in the cathodic current.

Electrical characterisations of the GaAs/Al structures are performed with a C (V) and I(V) automatic systems. The area of the contact is $S = 7.8.10^{-3} cm^2$.
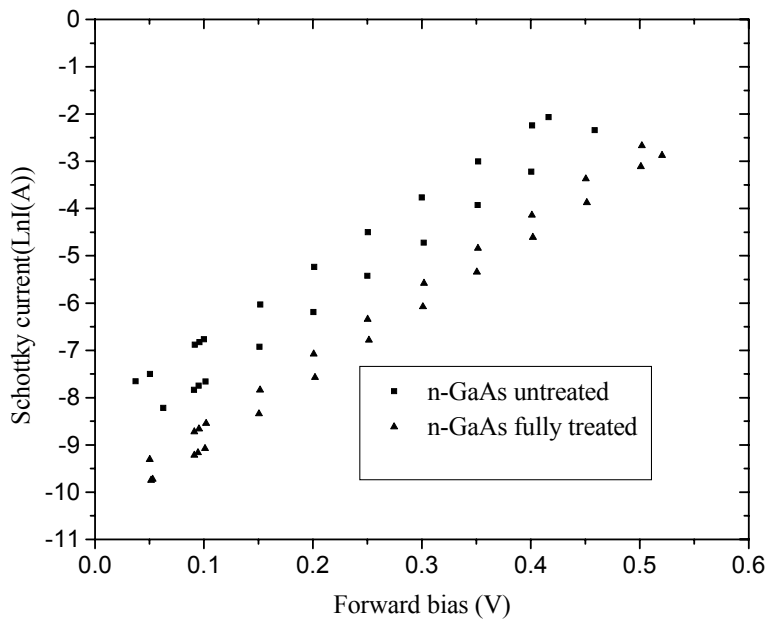

Fig. 3: Characteristics Ln(I) = f(V) of the untreated samples and treated (Al/n-GaAs).

Figure 3 shows Ln (I) versus V curves (n-GaAs/Al structures) where we can identify two zones. The first one, defined as the area between the solids squares, contains experimental curves (omitted in the figure for clarity) on untreated samples.The second one, which is bounded by solids ups triangles, contains curves for treated samples.
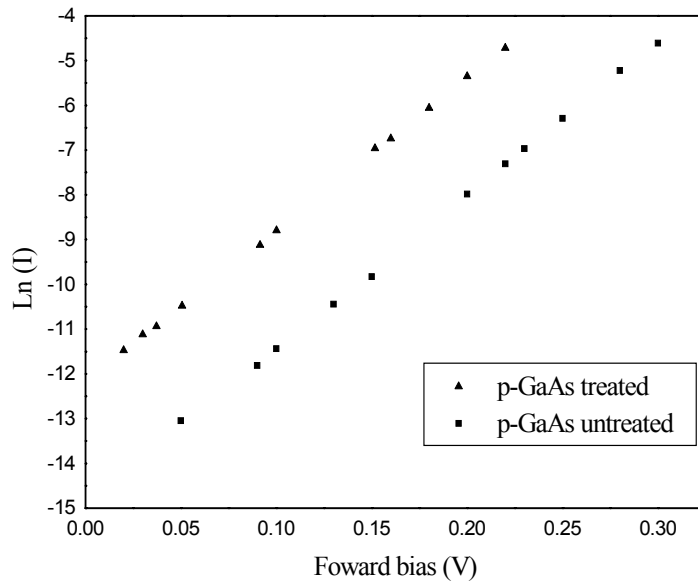

Fig. 4: Characteristics Ln(I) = f(V) of the untreated samples and treated (Al/p-GaAs).

Figure 4 shows Ln (I) versus V curves (p-GaAs/Al structures), the solids squares presented untreated samples and the solids ups triangles presented treated samples.
In each case, at least six samples were tested. The used ideality factor is between 1 and 1.2. We observe that the shift between the results for untreated samples and the results for treated samples leads to a variation of the interfacial barrier height – an increase for the n-type and an decrease for p-type.
The values of 1.11 and 1.12, for the ideality factor n of untreated and treated sample, respectively were obtained from the linear regions of the forward bias I–V plots.
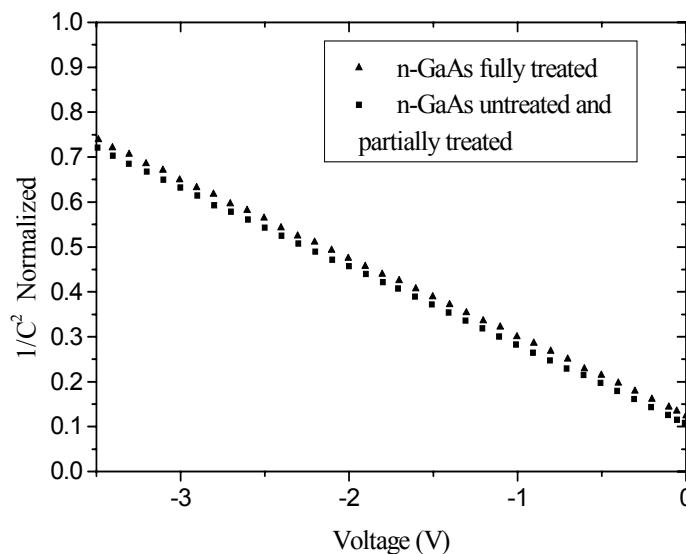

Fig. 5: 1/C^2 characteristics of untreated samples and treated (Al/n-GaAs).
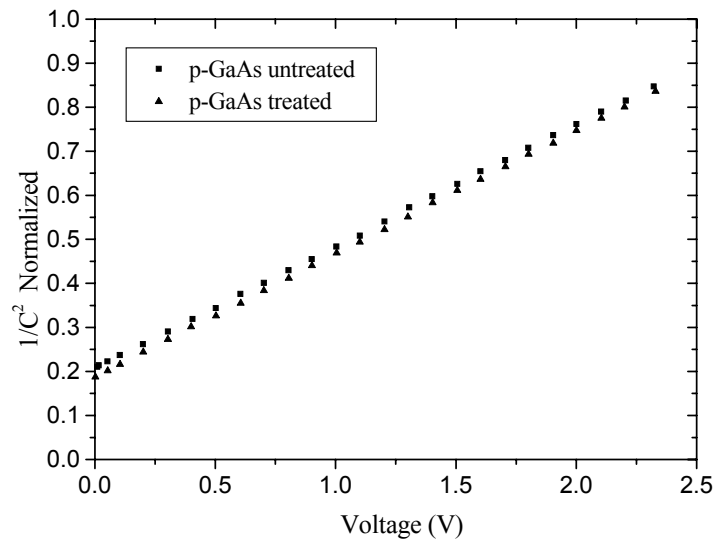
Fig. 6: $1/C^2$ characteristics of untreated samples and treated (Al/p-GaAs).

Figure 5 and 6 shows $1/C^2$ versus V curves obtained from C (V) measurements for treated and untreated n-GaAs/Al and p-GaAs/Al contacts. The doping concentration for n and p-type GaAs substrates – deduced from the slope of these curves – are in very good agreement with expected values. We may note that these curves are plotted from an average of results. The experimental threshold voltages for treated and untreated samples are very similar (within a range of less than 30 mV), thus the respective curves (solid square) are superimposed. The results for the Schottky barrier heights obtained for these same samples are also similar.

The shift of the treated sample curves (solid up triangle) is also shown in the figure and indicates a shift of the Fermi level at the treated interface.

We observe that the shift between the results for untreated samples and the results for treated samples leads to a variation of the interfacial barrier height – an increase for the n-type and decrease for p-GaAs/Al.

We have reported in table 1 and 2 a summary of our results. In all cases, the barrier height deduced from I(V) curves are shifted by about 60 meV from those obtained by C(V) measurements as it is usually observed by many authors [6].

Table 1: Typical parameters and results obtained after exploitation of I(V) and C(V) curves for n-GaAS.

Parameters	Untreated 1-2	Treated 1-2
Oxide thickness (Å)	20	4
Ideality factor n	1.117-1.123	1.127-1.129
Saturation current I_s (A)	5.7×10^{-9}-6.8×10^{-10}	$(2.8. -8.6) \times 10^{-11}$
Schottky barrier height ϕ_{bn} (eV) from I (V)	0.716-0.771	0.853-0.824
Schottky barrier height ϕ_{bn} (eV) from C (V)	0.8	0.9
Capacitance at $V_G = 0$ (pF)	465.35-465.35	426.66
grid area S (cm²)	7.85×10^{-3}	7.85×10^{-3}
Depletion layer width W (Å) at $V_G = 0$	1955.71	2133.05
doping concentration N_D (cm⁻³)	1.85×10^{16}	1.85×10^{16}
diffusion bias V_b (V)	0.72	0.82

Table 2: Typical parameters and results obtained after exploitation of I(V) and C(V) curves for p-GaAS.

Parameters	Untreated	Treated
Oxide thickness (Å)	20	4
Ideality factor n	1.117	1.127
Saturation current I_s (A)	3.538×10^{-7}	5.118×10^{-6}
Schottky barrier height ϕ_{bp} (eV) from I (V)	0.67	0.6
Schottky barrier height ϕ_{bp} (eV) from C (V)	0.6	0.51
Capacitance at $V_G = 0$ (pF)	392.512	416.025
grid area S (cm²)	7.85×10^{-3}	7.85×10^{-3}
Depletion layer width W (Å) at $V_G = 0$	2318.63	2187.58
doping concentration N_A (cm⁻³)	1.55×10^{16}	1.55×10^{16}
diffusion bias V_b (V)	0.517	0.447

The saturation current of treated n-GaAs/Al sample is almost two orders of magnitude less than the saturation current of untreated n-GaAs/Al sample.

The saturation current of treated p-GaAs/Al sample is almost one order of magnitude large than the saturation current of untreated p-GaAs/Al sample.

Substituting the values of the voltage dependence of n in Eq. (6) and using $\varepsilon_s = 12.8\varepsilon_o$, $\varepsilon_i = 3.5\varepsilon_o$, the values of N_{ss} versus E_c-E_{ss} is shown in Fig 7 for n-GaAs and versus $E_{ss}-E_v$ is shown in Fig 8 for p-GaAs. From these figures we can se an exponential increase of the density of interface states exists from midgap towards the bottom of the conduction band for n-GaAs and from midgap towards the high of the valence band for p-GaAs. This rise is less significant for untreated sample compared to treated sample. At any specific energy, the density of interface states of untreated sample is less than that of treated sample. Thus, most of the electrons will be injected directly into the metal forming a thermoionic emission current, while some of them are trapped by the interface states. This charge captures process results in an increase in the effective barrier height, thereby reducing the diode current for n-GaAs and in a decrease in the effective barrier height, thereby increase the diode current for p-GaAs [12-15].
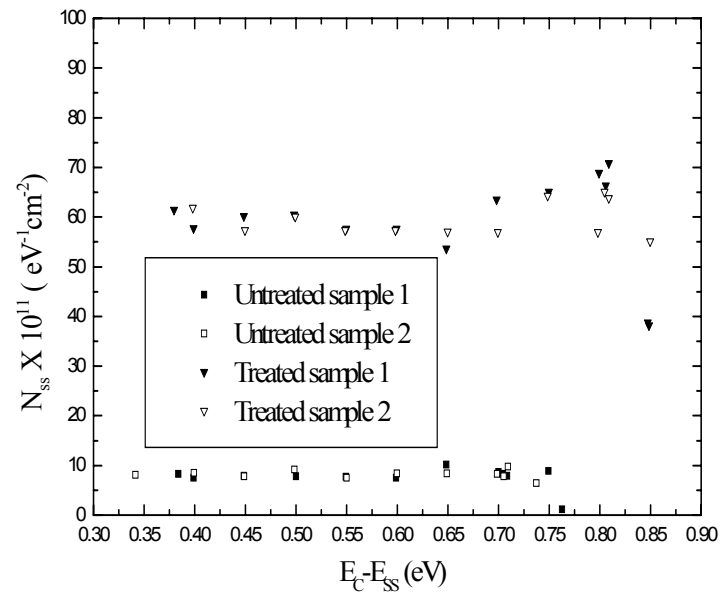
154

Fig. 7: Density of states versus ($E_C - E_{SS}$) of untreated and treated samples (Al/n-GaAs).
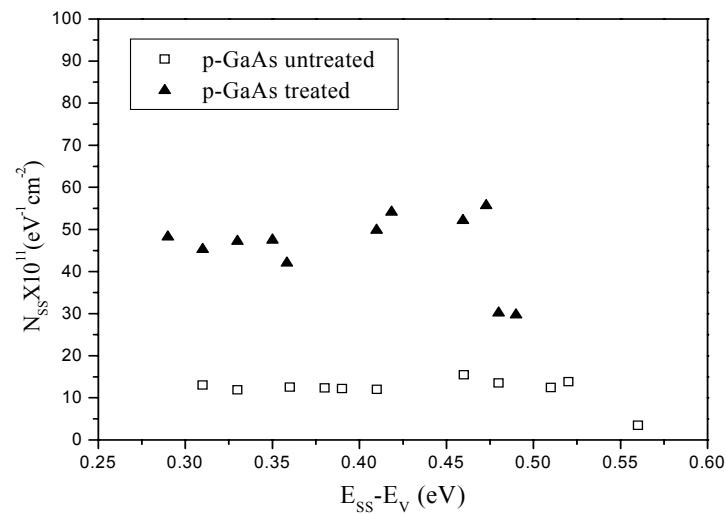

Fig. 8: Density of states versus ($E_{SS} - E_V$) of untreated and   treated samples (Al/p-GaAs).

We can conclude from these tables that treated samples exhibit a surface Fermi level located at 0.1 eV below the usual pinning position in GaAs/Al systems. We may also note that the samples not treated with selenid previous to ruthenium adsorption do not exhibit any Fermi level shift. Selenid is necessary for an electrically efficient adsoption of ruthenium.

These results, taken individually, may be interpreted by some of the models described in the literature. They provide evidence that the behaviour of such an interface is due neither to the sole properties of the semiconductor nor to those of the metal. It seems

necessary to take into account the chemistry of the interface. Additional experiments with a variety of metals are currently developed and would be helpful to better understand GaAs/metal contacts.

5. Conclusion

In experimental study, the potential barrier of the treated samples (ϕ_{BN} = 0,910V) is indeed superior to the potential barrier ϕ_{BN} of the untreated samples (ϕ_{BN} = 0,810V).

The Fermi level ($E_F = E_g-q\phi_{BN}$) has a tendency to get near the valence band after treatment.

We have found in fact that treatment shifts surface Fermi level to valence band and increases the density of surface states. We assume that generation recombination process occurring in the space charge region accounts for the observed kinetics of these states which behave a hole traps. We conclude that these treatments slightly increase (n-GaAs) barrier height in Schottky devices reducing their leakage current. The main interest of this treatment remains the enhancement of electronic transfer kinetics at GaAs electrolyte solution interface.

References

[1] W.E. Spicer, A. M. Green, J. Vac. Sci. Technol. **B11** (1993) 4

[2] H.C.Card, E.H. Rhoderick, J. Appl. Phys.D **4** (1971)

[3] J. Kolnik, M. Ozvold, Phys. Stat. Solidi (a) **122** (1990) 583

[4] C. Barret, A. Vapaille, Solid state electronics **19** (1976) 73

[5] M.K. Hudait, S.B.K rupanidhi, Mat. Scu. And Eng. **B87** (2001) 141

[6] E.H. Rhoderick, Metal semiconductor contacts, Oxford University Press Oxford (1978)

[7] H. Mazari, Z. Benamara, O. Bonnaud, R. Olier, Mat. Sci. And Eng **C21(**2002)307

[8] H. Mazari, Z. Benamara, N. Bachir Bouiadjra and O. Bonnaud, IMCES' 99, 16 & 17 May, University of Sidi Bel-Abbes (1999)

[9] H. Mazari, Z. Benamara, K. Ameur, O. Bonnaud, R. Olier, Madica Journées Maghreb-Europe, Hammamet, Tunisie, 29 Nov.-1st Déc. (2004)

[10] H. Mazari, K. Ameur , Z. Benamara, F. S. Bachir Bouiadjra, O. Bonnaud, R. Olier, International Congress on Photovoltaic And Wind Energy,Tlemcen-Algeria, 20-22 Déc (2003)

[11] H. Mazari, K. Ameur, Z. Benamara, F. S. Bachir Bouiadjra, O. Bonnaud, R. Olier, IX Journées Maghrébines des Sciences des Matériaux, Oran, Algérie, 8-10 may (2004)

[12] A. Turut, M. Saglam, H. Efeoglu, N. Yalcin, M. Yildirim, B. Abay, Physica **B205** (1995) 41

[13] S. Ashok, J.M. Borrego, R.J. Gutmann, Solid-State Electron. **22** (1979) 621

[14] M.K. Hudait, S.B. Krupanidhi, Solid State Electron **44** (2000) 1089

[15] A. Singh, J. Appl. Phys **68** (1990) 3475

[16] B.A. Parkinson, A. Heller, B. Miller , J.Electrochem.Soc. **126** (6) (1979) 954